

TERRITORIAL BEHAVIOUR OF BUZZARDS VERSUS RANDOM MATRIX SPACING DISTRIBUTIONS

GERNOT AKEMANN, MICHAEL BAAKE, NAYDEN CHAKAROV, OLIVER KRÜGER,
ADAM MIELKE, MEINOLF OTTENSCHMANN, AND REBECCA WERDEHAUSEN

ABSTRACT. The nearest and next-to-nearest neighbour spacings between buzzard nests in the Teutoburger Wald around Bielefeld, as gathered in the years 2000–2019, are compared with Ginibre random matrix ensembles as well as the Poisson spacing distribution in two dimensions. Our goal is a phenomenological description of some structural aspects in the territorial behaviour of these birds. To capture intermediate spacings between Ginibre and Poisson, we also compare to numerically generated two-dimensional Coulomb gases at different temperatures, which interpolate between the two. We find a stronger repulsion between nearest neighbours than between next-to-nearest ones, for more than the first half of the observed period. The increase of the absolute density of nests observed in that area over the monitored period of time leads to an increase of repulsion among neighbouring nests. Central to our approach is the use of well-established ideas from universal spatial structures, which suggest to employ a family of interpolating distributions with only one free parameter that parametrises the repulsion and that correlates well with the concepts from population ecology.

1. INTRODUCTION

In many animal and plant populations, reproductive success decreases with increasing population density. This density dependence of reproduction has been known since the dawn of modern animal ecology [1]. Although density dependence has been examined in different taxa [2], it is rather easily studied in large, territorial species. One particularly prominent group used for disentangling hypotheses about density-dependent reproductive success have been birds of prey [3, 4]. The predatory habit could amplify the occurrence of strong density dependence and make them especially suited for studies of the underlying mechanisms [5]. Territoriality allows density effects to be examined in detail, while this possibility could be impaired in classically colonial species. The charismatic nature, conspicuousness and relatively high vulnerability of birds of prey not only increase their conservation value, but also make recording of their reproductive success and population dynamics attractive and relatively common. They also offer the advantage of being very site-faithful and territorial: once they have occupied a territory, they rarely move and they are highly aggressive against intruders and hence territorial aggression can be fatal. The study of mechanisms that could explain the spatial clustering of bird of prey territories is therefore of great theoretical as well as applied value.

Here, the locations of buzzard nests collected in the years 2000–2019 in the Teutoburger Wald around Bielefeld are investigated. We are in the comfortable position to have about 100-200 nests per year available in this approximately two dimensional (2D) landscape, over a period of 20 years. Given such a data set, it is tempting to model the emergence and behaviour in space and time from an ecological point of view. However, this would mean to make many assumptions and to introduce even more parameters, which bears the danger of overfitting. Indeed, a less biased approach would begin by extracting structural properties from the data, such as distribution patterns, distance preferences,

Date: December 13, 2021.

or any kinds of correlations in space and time. Although the inference point of view from point process theory would be natural, compare [6], the data set does not seem to be large enough for such an endeavour. Consequently, the goal of this initial approach is rather modest in the sense that we primarily look at the spacing distribution between neighbouring points, that is, the nest locations.

A popular approach to spacing distributions is based on random matrix ensembles and enjoys a long history. It started independently in multivariate statistics [7], inspired from agriculture by Wishart, and in a statistical theory of energy levels of complex quantum systems by Dyson [8], motivated by Wigner and ideas of Bohr about the compound nucleus, see [9] for a historic account and various modern applications. Further examples without quantum mechanical background repeatedly show the signature of random matrix statistics, such as the spacing between subsequent buses in Cuernavaca (Mexico) [10], and parked cars or birds on a power line [11]. While most comparisons are made for data in one dimension (1D), comparing with the statistics of real eigenvalues of symmetric or Hermitian random matrices, few examples exist in 2D. Here, one is comparing with complex eigenvalues of random matrices without symmetries, with applications ranging from quantum chaotic systems with dissipation [12, 13], quantum field theory with chemical potential [14] to the spacing between chief towns of departments or districts [15] and Swedish pine trees [16]. Data sets similar to the latter two have been modelled by so-called determinantal point processes [17], for which random matrices provide a particular example.

In order to apply such ideas to the distribution of nests, we employ recent progress on the universality of certain distributions and start with a comparison to the distribution from a uniform Poisson process in 2D, which describes the distribution of uncorrelated points, and to the distribution of the complex Ginibre ensemble [18], which displays a rather strong repulsion. The repulsive nature is also easily detectable from the diffuse scattering components in the diffraction image of random point sets in 2D [19]. It should be emphasised that both distributions are parameter free, after fixing the normalisation and first moment to unity. As we shall see, the nest locations are indeed not adequately described by a Poisson process, in line with the known and frequently observed territorial repulsion of the buzzards.

In this first step, it also becomes clear that the repulsion in the Ginibre process is too strong, which is perhaps not too surprising either, as the ecological system should show some repulsion on a shorter scale (visual range), but not a long-range one. To deal with this situation, we embark on a simple one-parameter interpolation between Poisson and Ginibre statistics, which we derive from a known 2D Coulomb gas ensemble at variable temperature (being a non-determinantal, general Gibbs point process). While the underlying model has no direct meaning in the biological system, the parameter β (proportional to the inverse temperature) is taken as an *effective* phenomenological quantity and then determined by a simple fitting procedure. It directly measures the power of local repulsion $\sim s^{\beta+1}$ of two points at distance s .

It turns out that the employed one-parameter family of spacing distributions works well for the data. Moreover, our effective parameter proves sensitive to population density dependent properties, which indicates its suitability for our initial step in the data analysis.

2. OBJECT OF STUDY, DENSITY DEPENDENCE, AND TERRITORIALITY

The Common buzzard (*Buteo buteo* L.) is a medium-sized bird of prey (50–57 cm body length, 525–1364 g body weight) and breeds across the Palaearctic [20]. Its main prey consists of microtine rodents. A Common buzzard population comprising between 63 and 266 breeding pairs per year was monitored from 2000 to 2019 in an investigation area in Germany. The 300 km² area (8°25'E and

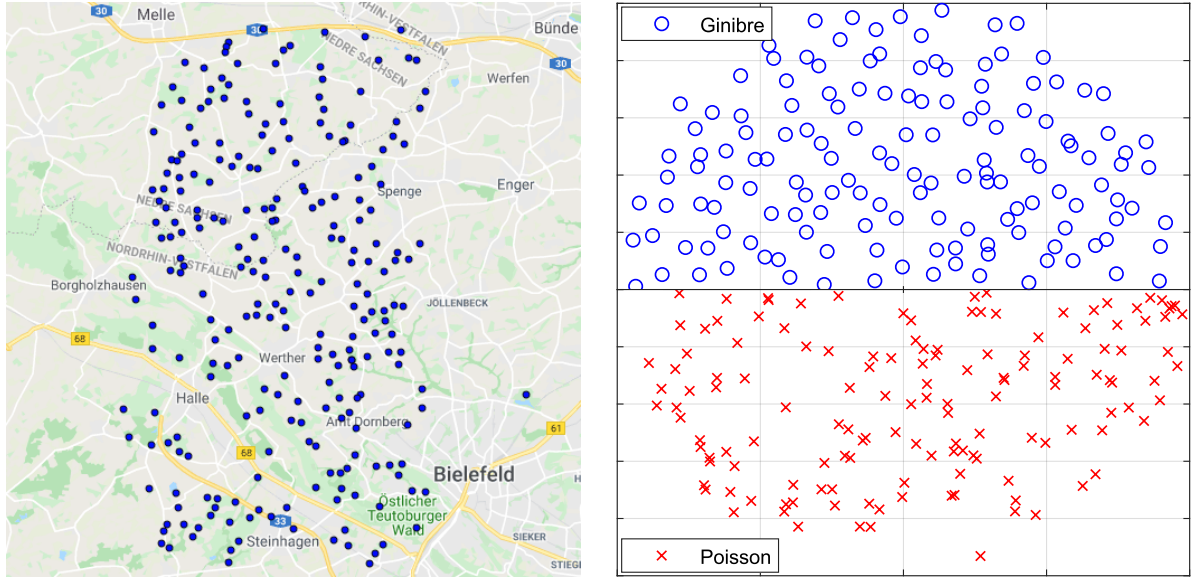


FIGURE 1. Visual comparison of Common buzzard nests and a snapshot of random matrix ensembles.

Left: Map showing the locations of 251 observed Common buzzard nests from the year 2019 north-west of Bielefeld. Note how smaller cities like Halle and Werther coincide with holes in the data. There are more nests outside the cluster shown here, but the position of these have not been recorded.

Right: Points distributed according to the 2D Poisson distribution (bottom, red crosses) and eigenvalues of a large complex Ginibre matrix (top, blue circles). Both ensembles consist of 300 points, the Poisson variables are generated uniformly on the unit disk, and the Ginibre variables are the eigenvalues of a complex Gaussian random matrix normalised to the unit disk. Only the top/bottom half disk is shown for an easier comparison. Notice how the Poisson points tend to cluster, whereas points from the Ginibre ensemble are more evenly spaced. This is reflected in the nearest neighbour spacing distributions (A.1) and (A.2), which we compare quantitatively to the Common buzzard nests below.

52°6'N) is located in Eastern Westphalia and consists of two 125 km² grid squares and 50 km² edge areas. The main habitat is the Teutoburger Wald, a low mountain region reaching a height of 315 m above sea level. Ridges are covered by Norway Spruce *Picea abies* and Beech *Fagus sylvatica*, with Oak *Quercus robur* and *Q. petraea* forests at lower altitudes. The second main habitat is a cultivated landscape to the north and south. In the north, forests are composed mainly of Beech and Oak, whereas Scots Pine *Pinus sylvestris* dominates in the south. The size of forest patches varies from rows of trees to large patches more than 10 km² in size and ca. 17% of the study site is forested. Most forests are less than 100 years old and the spruce forests are atypical of this region. This study site has been intensively monitored for Common buzzard and the resulting spatial data have been used extensively before [3, 21, 22].

All forest patches were visited in late winter to look for breeding pairs and all nests of four raptor species (Common buzzard, Goshawk *Accipiter gentilis*, Red Kite *Milvus milvus* and Honey Buzzard

Pernis apivorus) were recorded in either large-scale maps or GPS-devices to examine spatial distribution and interspecific competition. When an incubating Common buzzard was observed on the nest in both March and April, that pair was classified as breeding (in contrast to non-breeders which did not occupy a nest). An illustration is shown in the left panel of Figure 1.

Figure 1 shows the nest locations for a single year 2019, with the density among the highest of the total population. The effect of towns and smaller cities appears to be visible as holes in the data set. The statistics on the potential edge effects is too small to draw conclusions. We thus chose to treat all the data points as being part of a bulk, without considering edge effects. Notice that, within the Ginibre ensemble, the statistics at the edge of the spectrum (unit disk) differs from that of the bulk points. There, the transition from edge to bulk is very rapid though, within a distance of order $1/\sqrt{N}$ from the edge for N points.

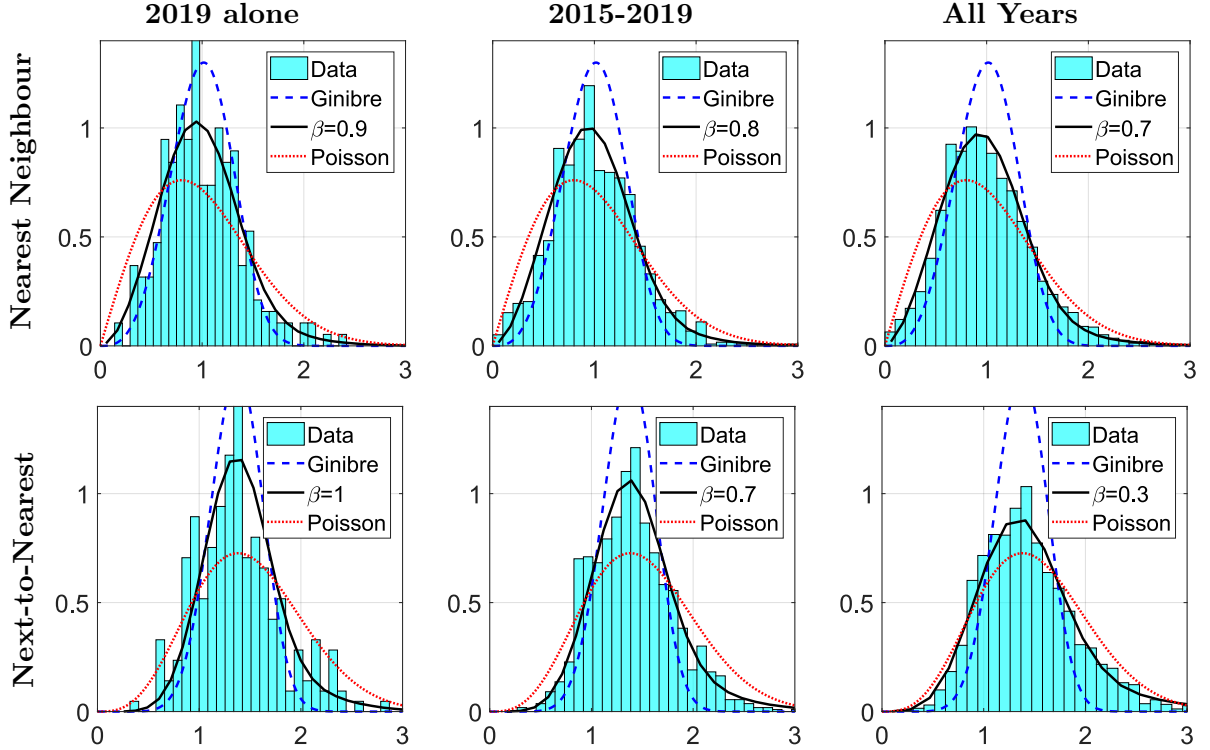


FIGURE 2. Comparison of distances between nests to those of a Coulomb gas (A.3) with a Kolmogorov fit, both nearest neighbour (NN) and next-to-nearest neighbour (NNN), where the repulsion β is treated as a fitting parameter. We have also added the curves corresponding to the analytic expressions for Poisson and Ginibre variables; see Equations (A.1) and (A.2), respectively. To illustrate our grouping of years, we provide the fit of a single year (left column), of 5 years (middle column), and of all 20 years (right column). Using one year, the fit quality is rather poor, but when using all years, we lose the temporal information. We therefore make a compromise through moving averages of 5 years. The result is shown in Figure 3. See also Figure 4 in Appendix C for the effects of different group sizes.

3. TERRITORIAL BEHAVIOUR OF COMMON BUZZARDS

Ideally, we wish to investigate the territorial behaviour over the years. Unfortunately, the individual years have too few data points for comparison; see Figure 2 (left) and Figure 4 (left) in the Appendix. We therefore group the nests in ensembles of 5 years (2000–2004, 2002–2005, ...). After unfolding the spectrum as explained in Appendix B, we fit the nearest and next-to-nearest neighbour spacings to a Coulomb gas with β as the fitting parameter describing the local repulsion; see Figures 2 and 3. Notably, these two fits do not give the same β . Let us first compare the β -dependence within each group. Initially, the next-to-nearest neighbour spacing gives a significantly lower value for β , which is about 1/2 of that of the nearest neighbour β -value. At first, it is close to the Poisson process at $\beta = 0$. This suggests that the correlation length is relatively small. That is, the Common buzzards are aware of their direct neighbours, but do not have considerable long-range interactions. This differs from the long-range interaction of the Coulomb force.

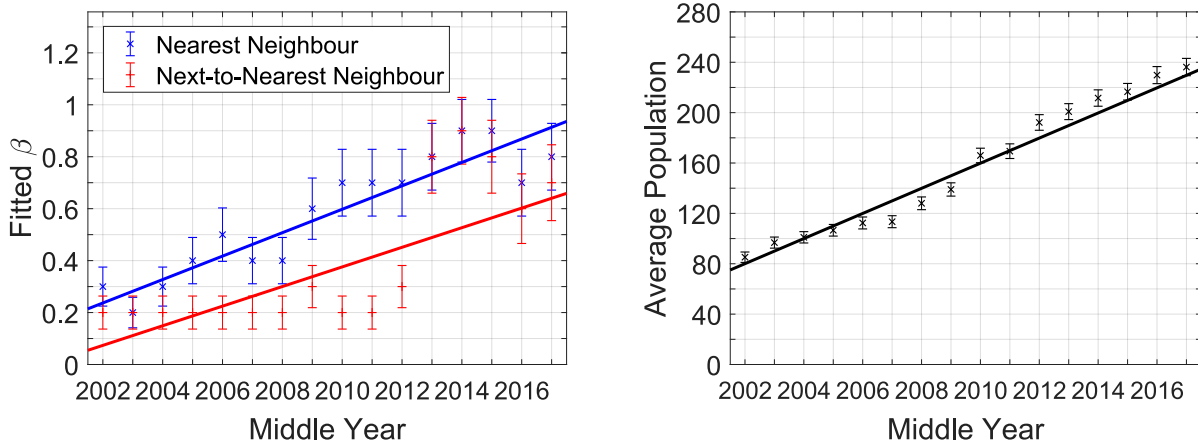


FIGURE 3. **Left:** Comparison of the nearest neighbour spacing distribution of all collected nests 2000–2019 to a Kolmogorov fit for the effective parameter β of the spacing distribution, obtained from a 2D Coulomb gas (A.3); see Appendix A. The fits to nearest (top blue data points) and next-to-nearest neighbour spacing (bottom red data points) are made in groups of 5 years. That is, the first group is 2000–2004 and the last is 2015–2019, compare with Figure 4 in Appendix C discussing different groups sizes.

As detailed in Appendix C, the statistical error bars are found by fitting the parameter β in the spacing distribution obtained numerically from the Coulomb gas (A.3) to themselves (bootstrapping), that is, the spread of the β obtained by fitting each of the 10^4 realisations to their average distribution. To avoid any influence from the choice of bin width for our data, we have in fact fitted to the cumulative distribution of the spacing distribution, using the Kolmogorov distance. A least-squares fit with a straight line is provided for both spacing distributions, to show the trend.

Right: The averages of the population size over the same groups of 5 years as well as a fit with a straight line. The errors of the individual years are here assumed Poissonian and propagated to the averages. Note that the linear increase in size coincides with the increase in β .

We then also compare the growth in population in Figure 3 (right) to the time dependence of the repulsion measured in β in Figure 3 (left) over the years and find that an increase in population coincides with an increase in repulsion. This is indicated by the linear fits in Figure 3. Note that the observed area is roughly the same through the years, so the population is proportional to the density. Surprisingly, beyond a certain critical density, the β -value of both spacings becomes comparable, indicating an increase in correlation length. For Coulomb gases, the normalised spacing distribution is invariant under a change in density, but here the added population makes the Common buzzards more territorial. This suggests that they care only about their closest neighbours, but not about the overall scale of the environment. In other words, there exists a length scale that is not present in the global potential of the Coulomb gas.

4. CONCLUSION AND OPEN QUESTIONS

We compared the spacing distributions of the nests of Common buzzards in an area of the Teutoburger Wald to a one-parameter family of correlated random variables that includes the behaviour of Poisson random variables and of complex eigenvalues of random matrices in limiting cases. We find that it provides a good effective description of the repulsion among neighbouring nests, thus quantifying the territorial interaction between the birds. This allows us to isolate population density effects over time, where we find an increase in repulsion through an increase of absolute population density, and to also gauge the correlation length of the interactions. We observe that the Common buzzards seem to care more about their nearest neighbours, while the next-to-nearest neighbours only become important beyond a certain population density.

One of the open questions is to come up with a simple phenomenological model that would lead to similar statistics as the one-parameter family of a 2D Coulomb gas that we found to be effective in the description of our data.

Acknowledgements: This paper grew out of a collaboration between members of three distinct research groups, all supported by the German Science Foundation (DFG), namely CRC1283 “Taming uncertainty and profiting from randomness and low regularity in analysis, stochastics and their applications” (GA and MB), IRTG2235 “Searching for the regular in the irregular: Analysis of singular and random systems” (AM), and CRC/Transregio 212 “A Novel Synthesis of Individualisation across Behaviour, Ecology and Evolution: Niche Choice, Niche Conformance, Niche Construction (NC)³” (OK). We thank Ellen Baake for useful discussions and careful comments on the manuscript, as well as the School of Mathematics and Statistics of the University of Melbourne for hospitality (G.A.).

APPENDIX A. SPACING DISTRIBUTIONS FROM POISSON, GINIBRE AND COULOMB GAS

Here, we recall the spacing distributions between nearest and next-to-nearest neighbours of correlated and uncorrelated random variables and discuss their relevance, related to the concept of universality in random matrix theory.

Let us begin with the uncorrelated case, the Poisson distribution (Poi). Given a set of uniformly distributed, uncorrelated points in 2D, the distances between nearest (NN) and next-to-nearest neighbours (NNN) follow the respective spacing distributions

$$(A.1) \quad \begin{aligned} p_{\text{Poi}}^{(\text{NN})}(s) &= \frac{\pi}{2} s e^{-\pi s^2/4}, \\ p_{\text{Poi}}^{(\text{NNN})}(s) &= \frac{\pi^2}{8} s^3 e^{-\pi s^2/4}, \end{aligned}$$

in the limit of large data sets. Here, both the zeroth and first moments are normalised to 1. Note that in contrast to 1D, where there is no repulsion among NN, uncorrelated points in 2D also seem to repel each other, with the linear factor stemming from the 2D area measure. For a concise derivation for such spacing distributions in D dimensions, see [23, Appendix A.2].

For correlated random variables, few instances exist where the spacing distribution can be computed analytically. Such an example is given by the complex eigenvalues of the Ginibre (Gin) ensemble [18]. It consists of complex non-Hermitian random matrices with independent Gaussian entries, with zero mean and variance $1/\sqrt{2}$, without further symmetry constraints. The complex eigenvalues of such matrices become correlated random variables, see (A.3) below for $\beta = 2$ for the joint density of eigenvalues, and the limiting spacing distributions at infinite matrix dimension are known, compare [12] for NN and [24] for NNN:

$$(A.2) \quad \begin{aligned} p_{\text{Gin}}^{(\text{NN})}(s) &= \left(\prod_{k=1}^{\infty} \frac{\Gamma(1+k, s^2)}{k!} \right) \sum_{j=1}^{\infty} \frac{2s^{2j+1} e^{-s^2}}{\Gamma(1+j, s^2)}, \\ p_{\text{Gin}}^{(\text{NNN})}(s) &= \left(\prod_{k=1}^{\infty} \frac{\Gamma(1+k, s^2)}{k!} \right) \sum_{j=1}^{\infty} \sum_{\substack{k=1 \\ k \neq j}}^{\infty} \frac{\gamma(1+j, s^2)}{\Gamma(1+j, s^2)} \frac{2s^{2k+1} e^{-s^2}}{\Gamma(1+k, s^2)}, \end{aligned}$$

where $\Gamma(1+k, s^2) = \int_{s^2}^{\infty} t^k e^{-t} dt$ and $\gamma(1+k, s^2) = \int_0^{s^2} t^k e^{-t} dt$ are the incomplete Gamma functions. The exact expressions at finite matrix size, where sums and products are truncated at $N-1$, converge very rapidly. For simplicity, we have not rescaled the expressions in (A.2) by the respective first moments, as is done in Figure 2. It is not difficult to see that, for small arguments, the repulsion is much stronger in (A.2), proportional to s^3 for NN and s^5 for NNN, compared to (A.1).

The limiting distributions (A.2) are universal in the sense that they hold beyond Gaussian distributions for independent matrix elements [25, 26]. Moreover, for all three Ginibre ensembles with real, complex, or quaternion matrix elements, the spacing distributions in the bulk (A.2) are the same [13, 27], which is why we display a single distribution for the Ginibre ensemble in Figure 2. This is in contrast to Hermitian random matrices with real, complex or quaternionic matrix elements, which lead to three different spacing distributions among the respective real eigenvalues; see e.g. [9].

We move to the model that allows us to interpolate between the Poisson and Ginibre distribution. It is given by a static gas of charged particles, repelling with respect to the long-range 2D Coulomb (Cou) interaction at inverse temperature $\beta = (k_B T)^{-1}$; see for instance [28]. To keep these particles together, they are put into a confining potential that we choose to be quadratic, $V(z) = |z|^2$. The joint probability density function of the N positions is then given by

$$(A.3) \quad p_{\text{Cou}, \beta}(z_1, \dots, z_N) = \exp \left[\beta \sum_{\substack{j, k=1 \\ j < k}}^N \log |z_k - z_j| - \sum_{j=1}^N |z_j|^2 \right],$$

where compared to standard conventions in statistical mechanics we have rescaled the positions as $\beta |z_j|^2 \rightarrow |z_j|^2$. This allows us to take the limit $\beta \rightarrow 0$ corresponding to uncorrelated variables,

which yields back the distributions (A.1). On the other hand, at $\beta = 2$, (A.3) agrees with the joint eigenvalue distribution of the complex Ginibre ensemble [18], with distributions (A.2). In this sense, the 2D Coulomb gas (A.3) provides a one-parameter family that interpolates between uncorrelated and random matrix behaviour of random variables in 2D. In the large- N limit, the global density of particles converges for all $\beta > 0$ to the unit disk, the so-called circular law, with height $1/\pi$ in our conventions for the area measure; see right panel of Figure 1. For local correlations such as the spacing distributions, the universality of the 2D Coulomb gas for arbitrary $\beta > 0$ is an open problem; see [29] for a detailed account.

Since no closed formula is known for the spacing for general $\beta > 0$, we compute the spacing distributions for NN and NNN numerically, with an importance sampling Metropolis–Hastings algorithm; see for instance [30, 31]. We have generated a library of distributions in steps of 0.1 for $\beta \in (0, 2)$ for our fits; see [13] for further details. Perturbatively, it is clear from (A.3) that the repulsion of NN increases polynomially, that is, $\lim_{s \rightarrow 0} p_{\text{Cou}, \beta}^{(\text{NN})}(s)/s^{\beta+1} \propto 1$ for small arguments; see Figure 2 for an illustration.

APPENDIX B. UNFOLDING OF THE SPECTRUM

Unfolding is a procedure to remove system-specific properties from spectral data, in order to extract local correlations that have a chance to be universal. For 1D, there is a unique, standard way to unfold, described for example in [9, Section 3.2.1]. In 2D, uniqueness is lost, see [14] for the criteria unfolding has to satisfy. Here, we will follow the approach established and successfully tested in [13] for 2D data.

The general problem in D dimensions can be stated as follows. The average spacing between two points close to a reference point z_0 is proportional to the inverse D -th root of the density at that point, $\rho(z_0)^{-1/D}$. Unfolding is a map that normalises the density (and thus the spacing distribution). It allows to remove the effect of the average (av) or mean spectral density $\rho_{\text{av}}(z)$, which is typically system-specific, and to separate it from the fluctuations (fl) around this density,

$$(B.1) \quad \rho(z) = \rho_{\text{av}}(z) + \rho_{\text{fl}}(z).$$

These fluctuations can often be described by simple, universal models, such as the predictions from Appendix A. In our 2D case, unfolding consists of a map of complex coordinates

$$z = x + iy \rightarrow z' = x' + iy'$$

to new coordinates, in which the new density is normalised, $\rho_{\text{av}}(x', y') = 1$. Following [13], we first approximate the average density $\rho_{\text{av}}(x, y)$ by a sum of smooth Gaussian distributions, as given in (B.2). Unfolding is then obtained by multiplying the distance of the NN (or NNN) to each point z_i by the factor $\sqrt{\rho_{\text{av}}(x_i, y_i)}$ in 2D. The resulting N unfolded spacings are collected, their density and first moment normalised to 1, and then compared to the correspondingly normalised distributions from Appendix A; see Figures 2 and 3. Notice that for points generated according to the Poisson, Ginibre, or Coulomb gas point process, the mean density is already flat for the values of N considered, see Figure 1 (right), and thus no unfolding is necessary.

The approximate mean density $\rho_{\text{av}}(x, y)$ is obtained by a sum of Gaussian distributions centred around each of the N data points z_j ,

$$(B.2) \quad \rho_{\text{av}}(x, y) \approx \frac{1}{2\pi\sigma^2 N} \sum_{j=1}^N \exp \left[-\frac{1}{2\sigma^2} |z - z_j|^2 \right],$$

where σ is the width, which is initially a free parameter to be chosen appropriately. In order to arrive at a smooth density $\rho_{\text{av}}(x, y)$, σ should be larger than the mean spacing \bar{s} between points. In [13], we tested this approximation for examples of random matrix ensembles where the mean density is not flat and the local spacing distribution is known to follow (A.2). There, the choice $\sigma = 4.5\bar{s}$ gave very good results, which is why we use the same value for the approximation (B.2), after determining the mean spacing \bar{s} for our data points for each individual year. The unfolded spacings for each year are then obtained by multiplication with the corresponding mean density $\sqrt{\rho_{\text{av}}(x_i, y_i)}$ at each data point z_j . These unfolded spacings are then put together in moving windows of 5 years, which are chosen large enough to have sufficiently many spacings (of the order of 1000) for a meaningful fit of the parameter β of the Coulomb gas (A.3).

Let us emphasise that the unfolding *removes* the trivial effect through the increase of the global population density observed in the period 2000–2019, and that the correlations among the unfolded points represent local properties that characterise the presence (or absence) of repulsion among data points.

APPENDIX C. FITTING APPROACH

We compare two distributions f and g with the Kolmogorov distance

$$(C.1) \quad D_{\text{KS}}(F, G) := \|F - G\|_{\infty} = \sup_x |F(x) - G(x)| \leq 1,$$

where F and G are the cumulative distributions of f and g , respectively. This has the advantage of being unbinned and takes into account that the distributions are normalised.

To estimate the error and to then make the linear fit of the population size and the repulsion strength β , we do the following. For the population size, we assume the numbers are Poisson distributed, where the width is the square root of the mean. The uncertainty on the average populations in the right plot of Figure 3 is found through error propagation, though these are merely there to guide the eye. As the grouped average population sizes are correlated, the linear fit is made with the individual years and plotted on top. See [32] for more on error estimation and statistics. For the Coulomb gas fit, this is non-trivial as the Kolmogorov fit does not give a clear connection to the uncertainty the same way a least-squares fit does. Because of the overlapping years in the moving average, the points are also correlated, and error propagation is not clear here.

We therefore employ a method called *bootstrapping*. We generate a number of Coulomb gas realisations with a true $\beta = \beta_0$ and make overlapping groups of 5 realisations the same way as we do with the moving average of the nests. By fitting the β of these realisations, we can estimate the error of the fitting method. The errors given in Figure 3 are the standard deviations of the fitted β for the corresponding β_0 . Because we group the realisations, we also have some information about the cross-correlation between the years. We extract this information by an average over groups of distance k between the midpoint for a given β_0 and call the correlation found here $V_k^{\beta_0}$. We do not represent the nests completely with this method, because we only group realisations of the same β_0 , but going into the individual β_0 of each year would defeat the purpose of grouping. Instead, to compare two groups with different β_0 and β_1 , we use the heuristic combination

$$(C.2) \quad V_k^{\beta_0, \beta_1} = \sqrt{\frac{(V_k^{\beta_0})^2 + (V_k^{\beta_1})^2}{2}}.$$

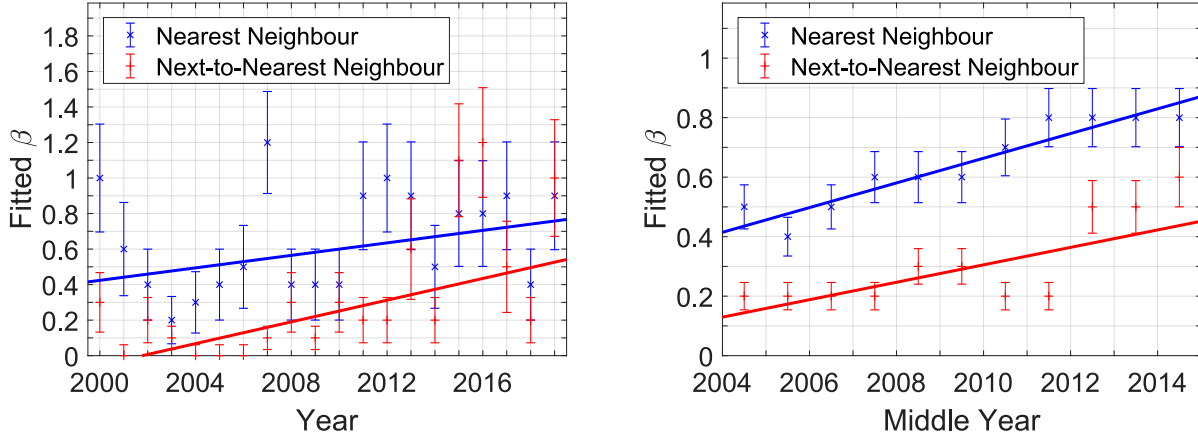


FIGURE 4. The effects of different group sizes. Plotted are the comparison of nearest neighbour and next-to-nearest neighbour spacing of all collected nests 2000–2019 to a Kolmogorov fit for the effective parameter β of the spacing distribution, obtained from a 2D Coulomb gas (A.3) in the same way as in Figure 3, but with different numbers of years per group.

Left: No grouping, that is, each year is fitted on its own. The fluctuations that arise when not grouping the years become apparent.

Right: Groups of 10 years. While the fluctuations are dampened, so is the change in β for next-to-nearest neighbour spacing for later years. Parts of the temporal structure is lost in this way. For this reason, we choose 5 years per group as a compromise.

We add them in quadrature to reflect the structure of the least-squares error, and the 2 in the denominator ensures that $V_k^{\beta_0, \beta_0} = V_k^{\beta_0}$. From here, we may construct the full covariance matrix of the grouped years in the left part of Figure 3. The off-diagonal elements turn out to be small compared to the diagonal elements, so the diagonal part illustrated as error bars in Figure 3 gives a reasonable idea about the uncertainty. The off-diagonal elements are, however, still included in the linear fit.

How many years are included in each group of course influences the results. We have chosen groups of 5, because this is a compromise where fluctuations are relatively small, but the temporal structure still is visible. See Figure 4 for the effect of different choices of group size.

REFERENCES

- [1] Lack, D. (1954). The natural regulation of animal numbers. Clarendon Press, Oxford, UK.
- [2] Sibly, R. M., Barker, D., Denham, M. C., Hone, J., and Pagel, M. (2005). On the regulation of populations of mammals, birds, fish, and insects. *Science* 309, 607–610.
- [3] Krüger, O., Chakarov, N., Nielsen, J. T., Looft, V., Grünkorn, T., Struwe-Juhl, B., and Møller, A. P. (2012). Population regulation by habitat heterogeneity or individual adjustment? *J. Anim. Ecol.* 81, 330–340.
- [4] Krüger, O. and Lindström, J. (2001). Habitat heterogeneity affects population growth in goshawk *Accipiter gentilis*. *J. Anim. Ecol.* 70, 173–181.
- [5] De Roos, A.M. and Persson, L. (2002). Size-dependent life-history traits promote catastrophic collapses of top predators. *Proc. Nat. Acad. Sci. USA* 99, 12907–12912.
- [6] Karr, A. F. (1991). *Point Processes and their Statistical Inference*, 2nd ed., Marcel Dekker, New York.

- [7] Wishart, J. (1928). The generalised product moment distribution in samples from a normal multivariate population. *Biometrika* 20 A, 32–52.
- [8] Dyson, F. J. (1962). Statistical theory of the energy levels of complex systems. *J. Math. Phys.* 3, 140–156.
- [9] Guhr, T., Müller-Groeling, A., and Weidenmüller, H.A. (1998). Random-matrix theories in quantum physics: common concepts. *Phys. Rep.* 299, 189–425 [arXiv:cond-mat/9707301].
- [10] Krbálek, M., Šeba, P. (2000). The statistical properties of the city transport in Cuernavaca (Mexico) and random matrix ensembles. *J. Phys. A: Math. Gen.* 33, L229–L234 [arXiv:nlin/0001015].
- [11] Šeba, P. (2009). Parking and the visual perception of space. *J. Stat. Mech.: Theo. Exp.*, 2009, L10002, 1–7 [arXiv:0907.1914].
- [12] Grobe, R., Haake, F., Sommers, H.-J. (1988). Quantum distinction of regular and chaotic dissipative motion. *Phys. Rev. Lett.* 61, 1899–1902.
- [13] Akemann, G., Kieburg, M., Mielke, A., Prosen, T. (2019). Universal signature from integrability to chaos in dissipative open quantum systems. *Phys. Rev. Lett.* 123, 254101, 1–6 [arXiv:1910.03520].
- [14] Markum, H., Pullirsch, R., and Wettig, T. (1999). Non-Hermitian random matrix theory and lattice QCD with chemical potential. *Phys. Rev. Lett.* 83, 484–487 [arXiv:hep-lat/9906020].
- [15] Le Caër, G. and Delannay, R. (1993). The administrative divisions of mainland France as 2D random cellular structures. *J. Phys. I*, 3, 1777–1800.
- [16] Le Caër, G. (1990). Do Swedish pines diagonalise complex random matrices? Internal Report, LSG2M (Nancy, 1990), unpublished.
- [17] Lavancier, F., Møller, J. and Rubak, E. (2015). Determinantal point process models and statistical inference. *Royal Stat. Soc. B* 77, 853–877 [arXiv:1205.4818 [math.ST]].
- [18] Ginibre, J. (1965). Statistical ensembles of complex, quaternion, and real matrices. *J. Math. Phys.* 6, 440–449.
- [19] Baake, M., Kösters, H. (2011). Random point sets and their diffraction. *Philos. Mag.* 91, 2671–2679. [arXiv:1007.3084].
- [20] del Hoyo, J., Elliott, A., and Sargatal, J. (1994). *Handbook of the Birds of the World. Vol. 2: New World Vultures to Guinea-fowl.* Lynx Edicions, Barcelona.
- [21] Chakarov, N., Boerner, M., and Krüger, O. (2008). Fitness in common buzzards at the cross-point of opposite melanin-parasite interactions. *Funct. Ecol.* 22, 1062–1069.
- [22] Müller, A. K., Chakarov, N., Heseke, H., and Krüger, O. (2016). Intraguild predation leads to cascading effects on habitat choice, behaviour and reproductive performance. *J. Anim. Ecol.* 85, 774–784.
- [23] Sá, L., Ribeiro, P., and Prosen, T. (2019). Complex spacing ratios: a signature of dissipative quantum chaos, preprint arXiv:1910.12784.
- [24] Akemann, G., Phillips, M. J. and Shifrin, L. (2009). Gap probabilities in non-Hermitian random matrix theory. *J. Math. Phys.* 50, 063504, 1–32 [arXiv:0901.0897].
- [25] Ameur, Y., Hedenmalm, H. and Makarov, N. (2011). Fluctuations of eigenvalues of random normal matrices. *Duke Math. J.* 159, 31–81 [arXiv:0807.0375].
- [26] Tao, T. and Vu, V. (2015). Random matrices: universality of local spectral statistics of non-Hermitian matrices. *Ann. Probab.* 43, 782–874 [arXiv:1206.1893].
- [27] Borodin, A., Sinclair, C. D. (2009). The Ginibre ensemble of real random matrices and its scaling limits, *Commun. Math. Phys.* 291, 177–224 [arXiv:0805.2986].
- [28] Forrester, P. J. (2010). *Log-Gases and Random Matrices.* Princeton University Press, Princeton.
- [29] Serfaty, S. (2019). Microscopic description of Log and Coulomb gases, in Borodin, A., Corwin, I., Guionnet, A. (eds.), *Random Matrices*, AMS, Providence, RI, 341–387 [arXiv:1709.04089].
- [30] Hastings, W. K. (1970). Monte Carlo sampling methods using Markov chains and their applications. *Biometrika* 57, 97–109.
- [31] Chafaï, D. and Ferré, G. (2019) Simulating Coulomb gases and log-gases with hybrid Monte Carlo algorithms, *J. Stat. Phys.* 174, 692–714 [arXiv:1806.05985].
- [32] Barlow, R. J. (1993). *Statistics.* Wiley, West Sussex, England.

FACULTY OF BIOLOGY, FACULTY OF MATHEMATICS AND FACULTY OF PHYSICS, BIELEFELD UNIVERSITY, P.O. BOX 100131, D-33501 BIELEFELD, GERMANY

E-mail address: akemann@physik.uni-bielefeld.de, mbaake@math.uni-bielefeld.de, oliver.krueger@uni-bielefeld.de, amielke@math.uni-bielefeld.de